Mass Spectrum and Thermal Behavior in Solid State of *N,N*-Di(1-hydroxyalkyl)-2-imidazolidinone

Choichiro SHIMASAKI,* Kyoko NAKAJIMA, Yuka SUGIMORI, Eiichi TSUKURIMICHI, and Toshiaki YOSHIMURA
Faculty of Engineering, Toyama University, Gofuku, Toyama 930
(Received January 12, 1989)

1,3-Bis(1-hydroxyalkyl)-2-imidazolidinones (**1**) were prepared by the reaction of imidazolidinone with propyl-, butyl-, isobutylaldehyde. They were unstable and moisture-sensitive substances, except for 1,3-bis(1-hydroxybutyl)-2-imidazolidinone (**1c**). In the decomposition by the electron impact of **1** and the dimer of **1c**, the molecular ion peak of **1** was not detected. The fragmentation of the imidazolidinone ring was considered to take place after a successive cleavage of the two side chains of **1**. The pyrolysis reaction of **1** was found to be a thermal decomposition via a molten state after a condensation reaction. The order of the pyrolysis was calculated on the basis of DSC curves. The condensation stage for **1c** apparently obeyed 1/2-order kinetics. From the dependence of the velocity on the temperature in DTA and the thermogravimetric analysis, the activation energy of decomposition was calculated; the value for the former was 67 and the latter 73 kJ mol^{-1}. The mechanism of pyrolysis was supported by the results of the IR spectrum and chemical analysis.

The derivatives of 2-imidazolidinone (**2**) have many advantages over any other substituted ureas. Furthermore, **2** has two active imino groups similar to the amino groups of urea. Compound **2** cannot produce compounds which have an intermolecular ether formation, such as tetrahydro-4*H*-1,3,5-oxadiazin-4-one. If **1** is cured at a certain temperature, the curing process must be similar to those of the main chain formation for the urea resin. The thermal decomposition of 1-hydroxyalkyl-2-imidazolidinone was previously reported by the present authors.[1] In this work, the decomposition study was extended to 1,3-bis(1-hydroxyalkyl)-2-imidazolidinone. The present authors investigated the condensation reaction of **1c** under no alkaline and acid catalyst conditions by IR, ^{1}H and ^{13}C NMR measurements. DSC and DTA are useful tools for measuring the thermally induced conformation transition of macromolecules as well as the polymerization process. An application of DSC and DTA to the study of polymerization provides information for kinetic data, such as the activation parameter.

Experimental

Materials. Compound **2**, ethanol, and methanol were of reagent grade and were used without further purification. The propionaldehyde, butyraldehyde, and isobutyraldehyde were distilled before use.

Preparation of Sample. 1,3-Bis(1-hydroxypropyl)-2-imidazolidinone (**1a**) was prepared according to the reported method for methylolurea.[2] The general procedure was as follows. *N*-(Hydroxymethyl)urea (**2** 21.5g (0.25 mol)) was suspended in 10 ml of ethanol under a nitrogen atmosphere. The ethanol solution was kept at pH 11 with a 8 M-NaOH aqueous solution (1 M=1 mol dm^{-3}) as the catalyst. After being stirred for 15 min, 35 ml of propionaldehyde was added dropwise to this suspension, which was kept under 15 °C by ice. White crude crystals were filtered with suction and dried in a desiccator. Recrystallization from chloroform gave white needle crystals of **1a**. 1,3-Bis(1-hydroxybutyl)-2-imidazolidinone (**1b**), and 1,3-di(1-hydroxy-2-methylpropyl)-2-imidazolidinone (**1c**) were prepared in a manner similar to **1a** by using 45 ml of butyr- or isobutyraldehyde and 10 ml of methanol.

Measurements. Elemental analyses of samples were carried out by using a Hitachi C,H,N-analyzer-026 at the Toyama Medical and Pharmacy University. IR spectra of samples were recorded on a Nipponbunko IR-810 using the KBr-disc method. The ^{1}H and ^{13}C NMR spectra of each solution was taken on a JNM-FX-90-FT-NMR instrument. A TMS was used as a reference. **1c** was dissolved in a deuterated dimethyl sulfoxide solution, and **1a**, **1b**, and **2** in a deuterated chloroform solution. A mass spectrum of each sample was taken with an ionization potential of 20 eV using a JEOL-JMS-D300 by EI method. Samples were heated in air using α-Al_2O_3 as reference by a Rigakudenki TG-DSC apparatus and Rigakudenki CN8078B2 (High Temperature Type) TG-DTA apparatus. DSC measurements were performed without using a reference by a Dupont 1090 DSC instrument.

Results and Discussion

Synthesis of 1. The physical properties of **1** are summarized in Table 1; the results from elemental analyses give the same values as those calculated. Most characteristic absorption in the IR spectra of **1** were identical. Only the absorption of **1** due to ν_{OH} (chelation) at about 3200 cm^{-1} was different among the three substrates. This absorption peak appears in the spectra of **1a**, **1b**, but not in **1c**. This result shows that only **1a** and **1b** have intramolecular hydrogen bonds. Figure 1 shows the possible schema A and B for the hydrogen bonding. From the fact that **1a** and **1b** decompose at lower temperatures than **1c**, it is suggested that *N*-(1-hydroxyalkyl)-2-imidazolidinone was formed by an elimination of aldehyde, provided that **1** has a structure of B. The absorption in the area 1680 cm^{-1} is sharp and shown in a single peak due to $\nu_{C=O}$. The absorption intensity of $\nu_{C=O}$ increases with increasing length of the side chain in **1**. In the mass spectra of **1**, the parent peak is not detected, but the peak of

Table 1. Physical Properties of **1a**, **1b**, and **1c**

		1a	**1b**	**1c**
	C	52.52(53.45)[a]	56.79(57.37)	57.52(57.37)
Elemental analysis/%	H	8.77(8.97)	9.67(9.63)	9.58(9.63)
	N	14.12(13.85)	12.29(12.16)	12.19(12.16)
Melting point/°C		101.9	96.5	131.8
Yield/%		62.0	94.0	98.0
IR spectra/cm^{-1}	ν_{OH}	3370	3350	3350
	ν_{OH} (chelation)	3200	3200	—
	ν_{CH}	2880, 2970	2870, 2970	2870, 2970
	$\nu_{C=O}$	1680	1685	1665
	ν_{C-O}	1080	1100	1040
^1H NMR position/ppm	In ring			
(Relative intensity: multiplicity)[b]	$-(CH_2)_2-$	3.387(4H : m)	3.339(4H : m)	3.234(4H : m)
	In substituent group			
	$-CH_3$	0.917(6H : t)	0.960(6H : d)	0.769, 0.947(6H : d)
	$-CH_2-$	1.627(4H : m)	1.459(8H : m)	—
	-CH-	5.191(2H : m)	5.388(2H : m)	1.722, 4.676(2H : m)
	-OH	4.557(2H : d)	4.894(2H : d)	5.482(2H : d)
^{13}C NMR	In ring			
	$-(CH_2)_2-$	36.730	36.795	35.958
	C=O	161.277	159.752	159.923
	In substituent group			
	CH_3	9.832	13.773	18.503, 19.234
	$-CH_2-$	26.708	18.491	—
	-CH-	77.632	82.740	80.375, 31.155

a) Calculated values in parentheses. b) d: doublet, t: triplet, m: multiplet.

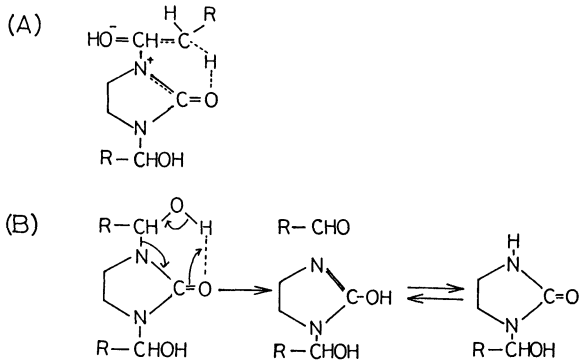

Fig. 1. Structure of A and B for **1**.

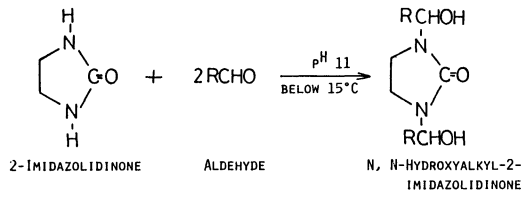

R : CH_3CH_2- **1a**

$CH_3(CH_2)_2-$ **1b**

$(CH_3)_2CH-$ **1c**

Scheme 1.

$(M-2H_2O)^+$ is detected as a base peak. The analytical and spectroscopic data in Table 1 indicate that the structure of **1** is the same as that proposed in Scheme 1.

The Fragmentation Mechanism for 1. The main cleavage mechanism for **1a** and **1b** is shown in Figs. 2 and 3, respectively. The molecular ion peak for both samples could not be detected. A very characteristic peak in both samples is the $(M-2H_2O)^+$ peak, which is the base peak. The elimination of the methyl group arises from one substituent group which is

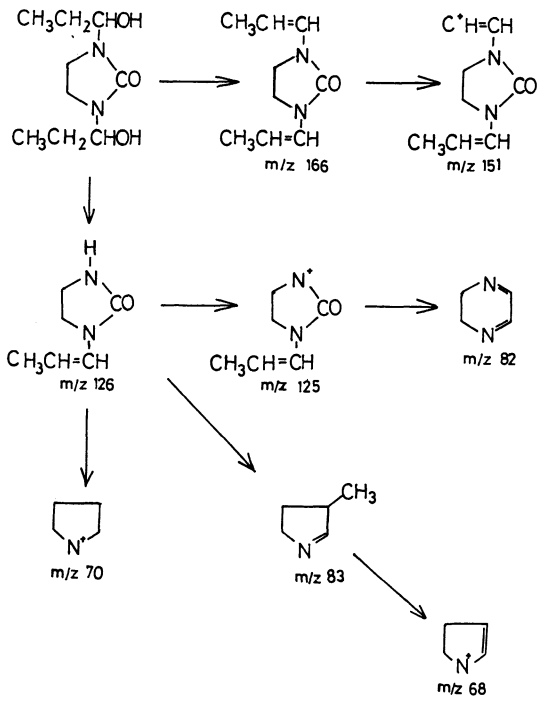

Fig. 2. The main cleavage mechanism for **1a**.

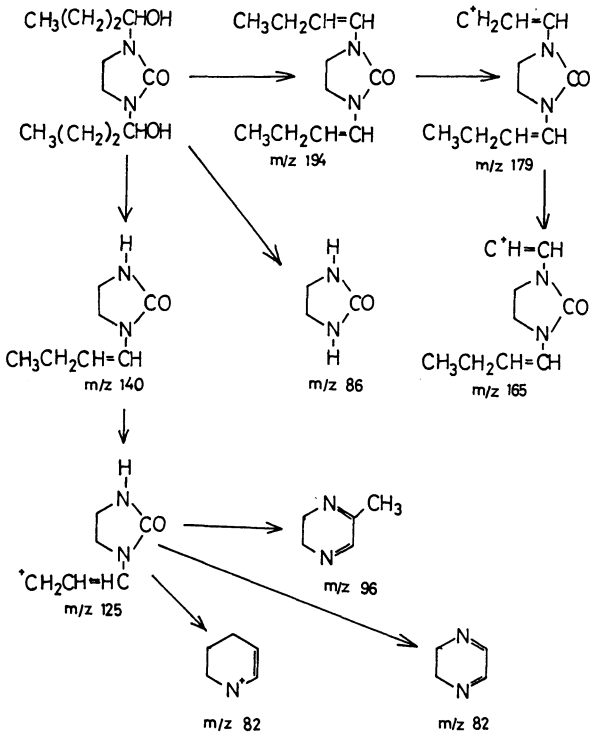

Fig. 3. The main cleavage mechanism for **1b**.

present in the base peak. The peaks at *m/z* 151 and 179 for **1a** and **1b** are the results of the ions from those base peaks. Although small in size, the peaks at *m/z* 126 and 140 for **1a** and **1b**, respectively, are due to a fragment ion resulting from the loss of aldehyde and water from the two substituent groups. The peak at *m/z* 125 appeared in both samples. In **1a**, this peak is due to the fragment ion resulting from the loss of the 1-hydroxypropyl group and water from the two substituent groups. In **1b**, this peak is due to the fragment ion resulting from the loss of propionaldehyde, water, and ethyl group from the two substituent groups. The peak due to the formyl group (*m/z* 58 or 72) and that due to the hydroxyl group (*m/z* 59) have been detected. From the fragment ion peaks at *m/z* 126 and 125, the functional group such as a carbonyl group, cyanic acid, and methyl group seems to be eliminated easily. In addition, the peak due to the elimination of two formyl groups (*m/z* 86) for both samples is also detected.

Figure 4 shows the detailed cleavage mechanism from the starting fragment ion at *m/z* 125 of **1b**. There are three cleavage patterns: I, II, and III. Considering the high resolution for the identification of the atomic content of the ions, it was concluded that fragmentation in I and II occurred through the loss of the carbonyl group, while III followed from the loss of HNCO (cyanic acid); the former fragmentation ion is

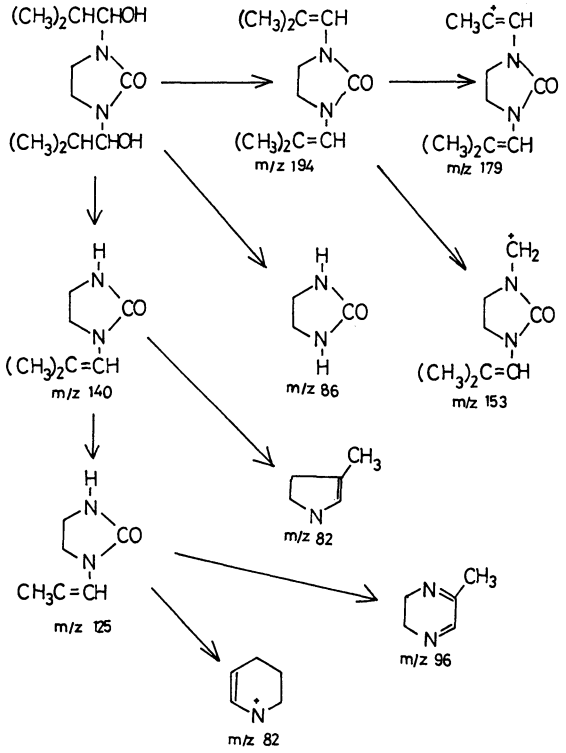

Fig. 5. The main cleavage mechanism for **1c**.

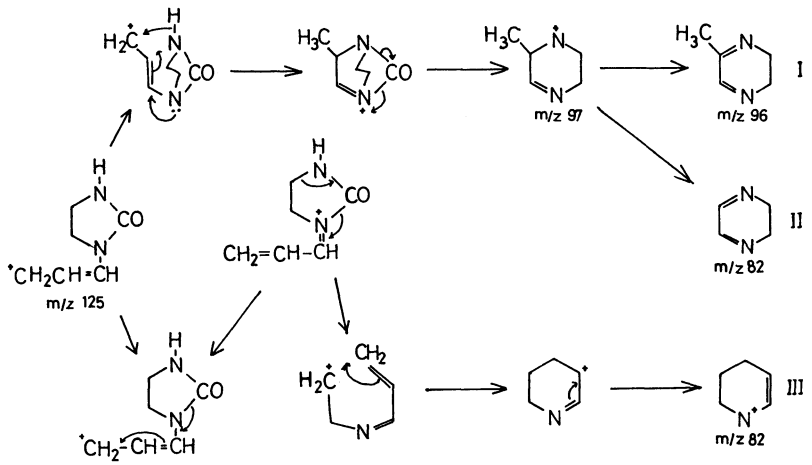

Fig. 4. The detailed cleavage mechanism for **1b**.

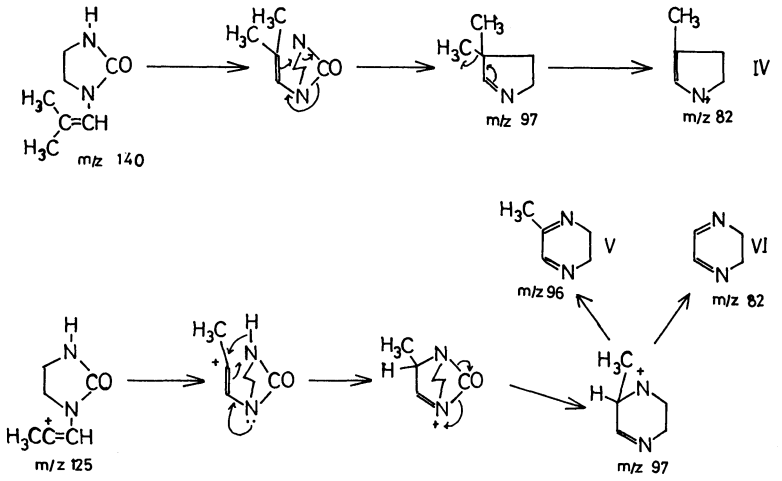

Fig. 6. The detailed cleavage mechanism for **1c**.

due to $C_5H_9N_2$ at m/z 97, the latter is C_5H_8N at m/z 82. The difference of cleavage patterns in I and II was confirmed by evidence from the high-resolution mass spectrum at m/z 96 and 82, which corresponds to fragment ions $C_5H_8N_2$ and $C_4H_6N_2$, respectively. These fragment ions are formed by the loss of proton and methyl groups from the ion at m/z 97.

The main cleavage mechanism for **1c** is shown in Fig. 5. The fragment ion detecting in **1c** is similar to that obtained for **1b**. Figure 6 shows the detailed cleavage mechanism from the starting fragment ions at m/z 140 and 125. Also, there are three cleavage patterns, such as IV, V, and VI. The IV cleavage pattern is confirmed from the fact that the fragment ions, $C_6H_{11}N$ (m/z 97) and HCNO (m/z 43) were detected, and, furthermore, the ion resulting from the loss of methyl group in the former fragment ion at m/z 97 was identified. The V and VI cleavage patterns are similar to I and II in Fig. 4, respectively.

Thermal Analysis. Figure 7 shows TG-DSC curves for **1**. These DSC curves exhibited an endothermic and an exothermic peak. The endothermic peak is attributed to both molten and condensation for **1**. However, the exothermic peaks for **1** are not always clear over a wide temperature range. The TG curve shows that the pyrolysis process for **1** takes place in two stages. In Fig. 7, the first plateau of the TG curve is probably due to a condensation of **1** to a dimer compound. The other plateau corresponds to a thermal degradation and a decomposition reaction. The TG-DSC measurement for **1c** was carried out at five heating rates from 0.625 to 20 °C min^{-1}. Figure 8 shows the DSC curves of **1c**. As shown in Fig. 8, both, the primary and secondary peak of the DSC curves shifted to higher temperature as the heating rate increased. At a heating rate of less than 10 °C min^{-1}, a new sharp peak appears in the area of 130 °C between the primary and secondary peak. **1c** melts rapidly at 132 °C. According to this fact, this sharp peak may be due to a molten stage. However, the

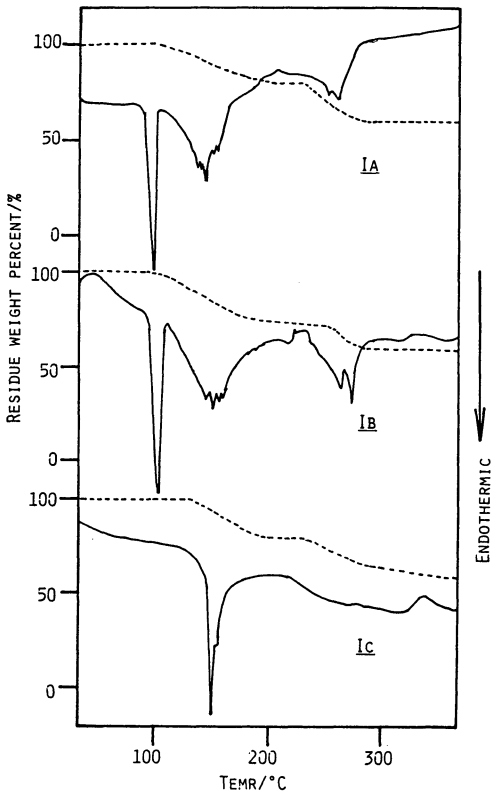

Fig. 7. TG-DSC curves for **1**.

fraction of the residual weight around 130 °C has a value approximated to that of the (molecular weight of **2**)/(molecular weight of **1c**) ratios. Since the melting point of **2** is 131 °C, this molten stage may not be due to the melting point for the eutectic mixture, but for **2**. Furthermore, TG-DTA measurement for **1c** was carried out at the heating rate from 2 to 10 °C min^{-1}. Both the primary and secondary peaks of the DTA curves shifted to higher temperatures with an increase in the heating rate, similarly to the DSC curves.

Kinetic Discussion for 1c. The kinetic discussion

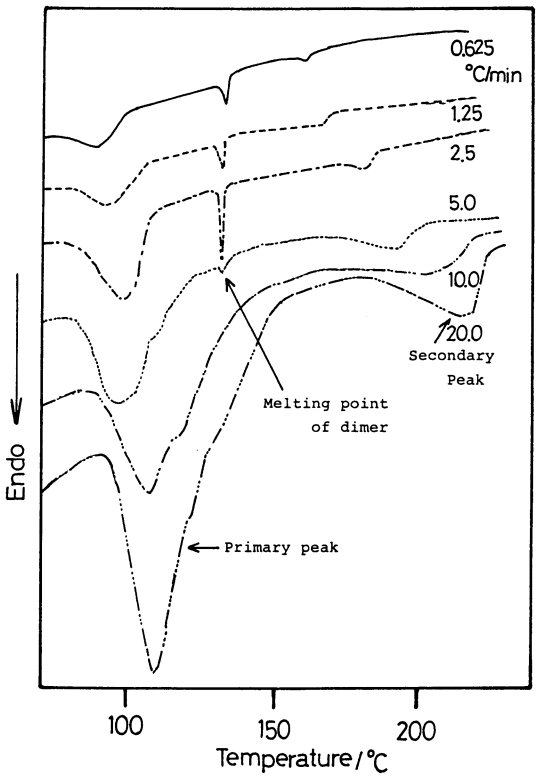

Fig. 8. DSC curves for **1c** at various heating rates.

is carried out in terms of the thermal analysis. Two methods for obtaining kinetic parameters from TG-DTA curves were applied. These methods are based on the general form of kinetic formulae and are applicable to general types of relation governed by a single activation energy. One method by Ozawa[3] utilizes the linear relation between the reciprocal of the absolute temperature and a definite fraction of the weight loss and the heating rate in TG curves in order to estimate the activation energy. The other method by Kissinger[4] requires information concerning both the temperature of the maximum peak and the heating rate in DTA curves; the Kissinger's plot is made for an apparent activation energy. According to Ozawa's method in thermal analysis, we carried out observations of the change in TG curves by different heating rates (ϕ). In each definite fraction of weight loss (θ), this method utilizes a linear relation between the reciprocal of the absolute temperature and the ordinal logarithm of the heating rate. The structural quantity is assumed to change the following ordinary reaction kinetics:

$$\theta = \Delta E/\phi R \cdot \rho(\Delta E/RT), \tag{1}$$

where ΔE and R are the activation energy and the gas constant, respectively. Also,

$$\log \rho(y) \simeq -2.315 - 0.4567y \quad (20<y<60). \tag{2}$$

Thus,

$$\log\phi_1 + 0.4567\Delta E/RT_1 = \log\phi_2 + 0.4567\Delta E/RT_2 = \cdots\cdots . \tag{3}$$

When an ordinary logarithm for a heating rate in Eq. 1 as the abscissa and the reciprocal of the absolute temperature as the ordinate is plotted, we obtained a straight line. From the gradient of this straight line, corresponding to $-0.4567\Delta E/R$, the activation energy was obtained.

It is evident, therefore, that the variation of the peak maximum for DTA curve can be expressed by means of an equation of the form

$$-\Delta E/R = \Delta\log(\phi/T_m^2)/\Delta(1/T_m), \tag{4}$$

where ϕ stands for the heating rate; ΔE, for the activation energy; T_m, for the temperature of the DTA-maximum; and R, for the gas constant. This method utilizes the linear relation between the $\Delta(1/T_m)$ and

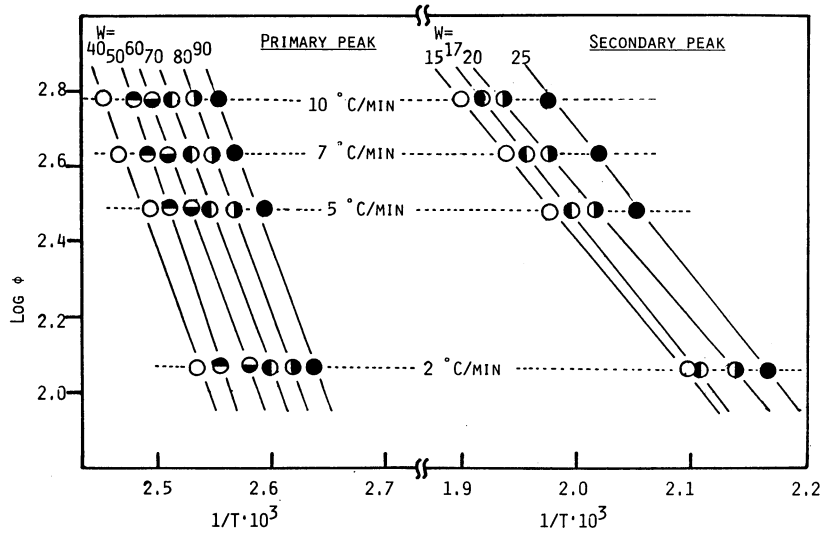

Fig. 9. Plots of logarithms of heating rate versus the reciprocal of absolute temperature for given conversation of pyrolysis of **1c**.

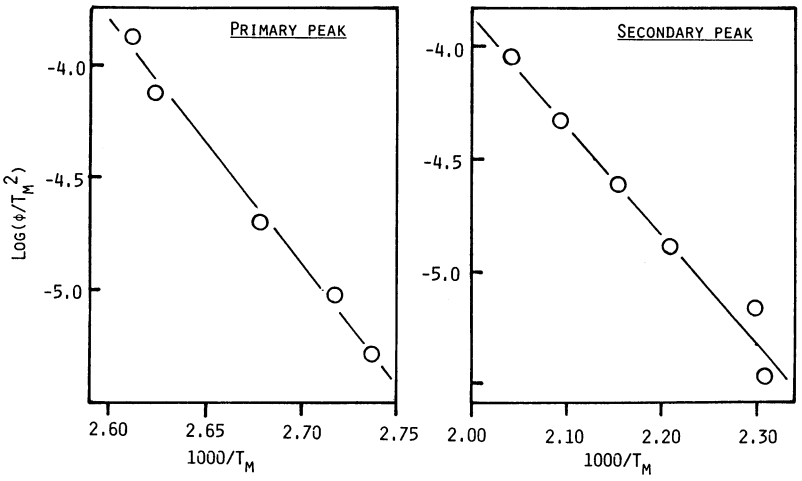

Fig. 10. Kissinger's plots for **1c**.

Table 2. The Apparent Activation Energy by TG and DTA Method of **1c**

Reaction process	Activation energy/kJ mol^{-1}	
	TG method	DTA method
Polycondensation	67	73
Pyrolysis	150	145

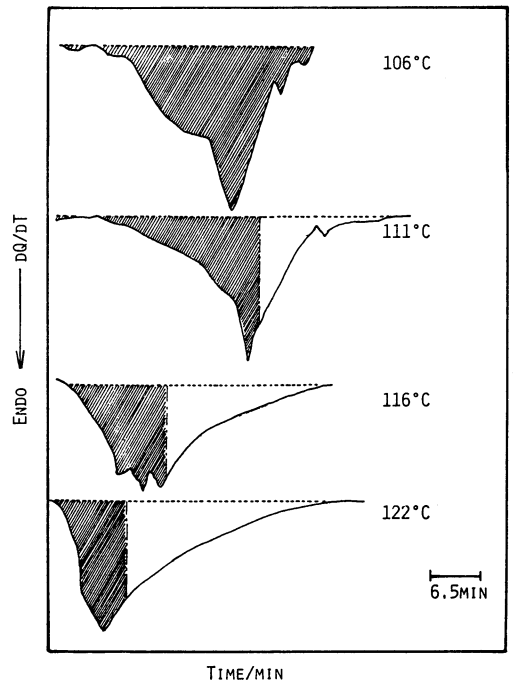

Fig. 11. Isothermal pyrolysis curves of **1c** at various temperatures.

$\Delta\log(\phi/T_m^2)$. For these TG and DTA curves, Ozawa's or Kissinger's plots of **1c** were linear. Figures 9 and 10 show the results of these plots. Table 2 shows the values of the activation energy which was calculated from these plots.

Next, a kinetic study was carried out in terms of McGhie method.[5] DSC measurements were carried out over the temperature range 105—120 °C by a method in which the sample was hermetically sealed in an aluminum pan and in a DSC cell using an isothermal mode. Figure 11 shows typical isothermal condensation curves for **1c**. This kinetic study of the pyrolysis process of **1c** was carried out for the shaded parts with the same heat quantity. The 1/2-order kinetics plot of $2\times[a^{1/2}-(a-x)^{1/2}]$ vs. $t-t_0$ for each curve is linear, where a is the area under a given isothermal curve, and x is the fractional area up to time t. Figure 12 shows these plots for isothermal reactions of four samples at 106, 111, 116, 122 °C. The data have been normalized with respect to time by plotting the time after an induction period of t_0. Thus, each isothermal curve yielded two important quantities, t_0 and k. The kinetic data for the condensation of **1c** are summarized in Table 3.

Table 3. Rate Constants and Kinetic Data for the Polycondensation Process of **1c**

a) Rate constants

T/K	Rate constant, k/mol$^{1/2}\cdot$l$^{-1/2}\cdot$s^{-1}
379	0.978×10^{-2}
384	1.372×10^{-2}
389	1.661×10^{-2}
395	2.367×10^{-2}

b) Kinetic data

A/mol$^{1/2}\cdot$l$^{-1/2}\cdot$s^{-1}	E_a/kJ$\cdot$mol^{-1}	ΔH/kJ$\cdot$mol^{-1}	ΔS/e. u.
1.62×10^{7}	68	64	28

Thermal Condensation of 1c. The thermal condensation of **1c** was considered from the results of IR spectra, ^{1}H and ^{13}C NMR spectra, mass spectra, and elemental analysis. **1c** was heated for various times under isothermal, or at various temperatures, under a nitrogen atmosphere in a thermostat. The IR spectra of the condensation product for **1c** show that the absorption due to ν_{C-O} at about 1100 cm^{-1} decreases in intensity. When the heating time was changed, the

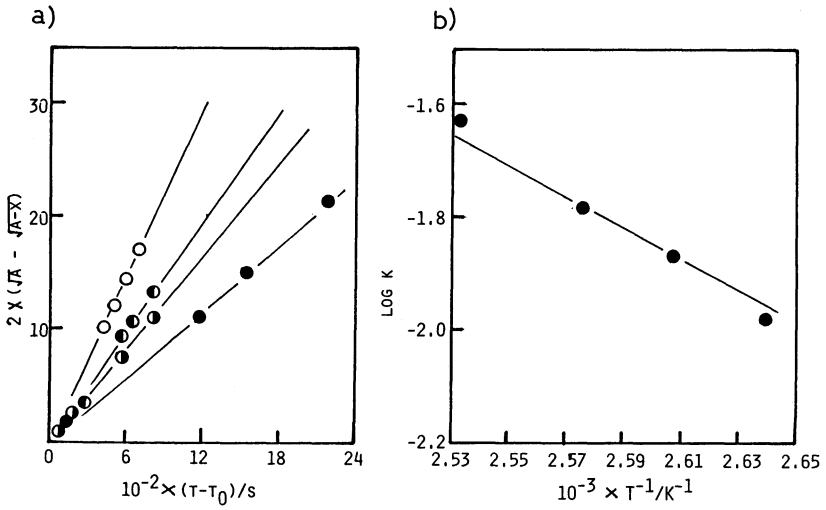

Fig. 12. a) 1/2 order kinetic plots of $2\times[a^{1/2}-(a-x)^{1/2}]$ vs. $t-t_0$ for the isothermal polycondensation of **1c**. b) Arrehenius plots of the 1/2 order kinetic constant for the polycondensation of **1c**.

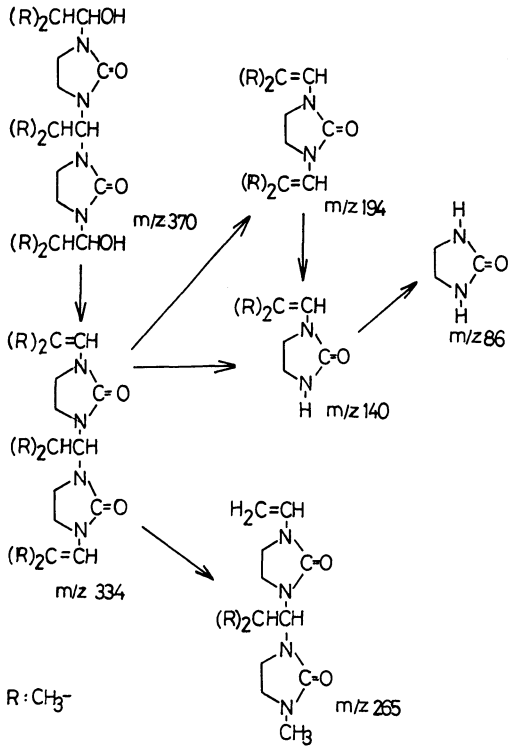

Fig. 13. Main fragmentation for dimer of **1c**.

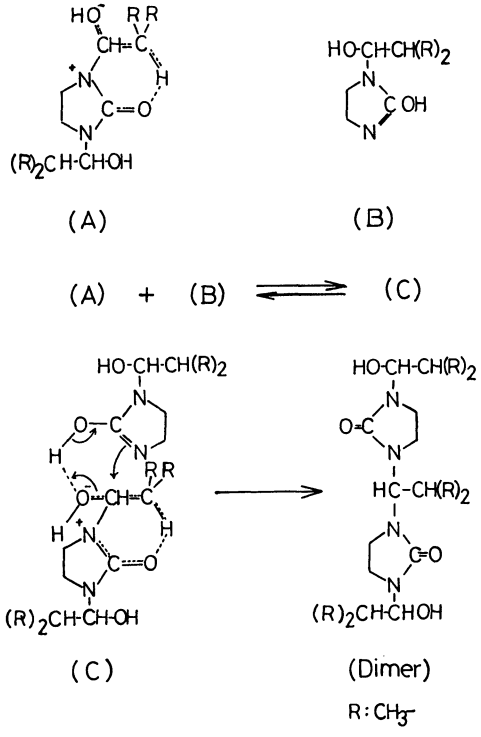

Fig. 14. The dimerization process for **1c**.

absorption peak due to $\nu_{C=O}$ at about 1680 cm^{-1} shifted to larger wavenumber with increasing time. The peak due to $\nu_{C=O}$ shifted at 1700 cm^{-1} after heating it for 5 h. The absorption peak due to ν_{OH} decreased in intensity with increasing heating time. On the other hand, when the temperature was changed, the heating product at 110 °C showed similar changes after 5 h. Also, the absorption peak due to ν_{NH} in the neighborhood of 3400 cm^{-1} appears at 145 °C. From these results it seems that both dehydration and condensation occur simultaneously for the thermal reaction of **1c**. The ^{13}C NMR spectra of **1c** shows that the signal at δ 159.923, due to the carbonyl group, separates into two signals, and that the signal due to the α-carbon atom attached to the hydroxyl group splits into three parts after condensation. These results show that the formation process of the dimer seemed to be dehydration after intermolecular hydrogen bonding. In the ^1H NMR spectra of **1c** and its condensation product, it was observed that the signal due to the hydroxyl group disappeared after condensation. The mass spectra of the condensation products also support this dimer

formation. There are no peaks due to trimer or oligomer in these mass spectra. The observed fragment ions in the mass spectra of the condensation products support the main fragmentation mechanism of the dimer in the case of **1c**. In the mass spectra after heating for 5 h, a peak at m/z 334 was detected. This peak is due to the fragmentation ion peak which is formed by the loss of two moles of water from molecular ion (M^+). The peak due to a molecular ion which is a dimer of **1c** was not detected. The maximum mass number ion peak obtained for these mass spectra, was the peak at m/z 265. The obtained fragment ion peak was cleared by considering the high-resolution mass spectra for an identification of the atomic content of the ions. Figure 13 shows the main cleavage mechanism of the dimer in the case of **1c**.

Reaction Mechanism for Thermal Condensation of 1c in Solid State. The possible structure of intermediates formed during the activated state in the course of the dimerization process for **1c** is the activated complex (A) and the enol type (B), like lactim in Fig. 14. The presence of (A) was confirmed by ESR measurements[1)] in the case of 1-mono(1-hydroxyalkyl)-2-imidazolidinone; (B) gave no direct evidence concerning its existence in the solid state. In the molten state, however, the (B) had likewise been formed in the case of cyanuric acid. By a comparison of structures (A) and (B), the hydroxyl group of (A) was easier to eliminate than that of (B). In the next step, the activated complex (C) (Fig. 14) was formed from (A) and (B). It is expected for **1c** that the DSC measurement was taken in order to obtain information regarding the formation of (C) to the dimer. From these results, it is clear that (A), (B), and (C) are formed during the induction period.

We wish to thank Miss Misao Shinoda for the Mass spectra and Mr. Yoshiharu Yoneyama for NMR measurements. We thank Prof. Shigeya Takeuchi for good advice regarding DSC measurements.

References

1) C. Shimasaki, R. Kanayama, H. Yoshida, and M. Yugamidani, *Bull. Chem. Soc. Jpn.*, **60**, 193 (1987).
2) S. Takeuchi, "Yukikagobutsugoseiho," ed by Yukigosei Kagakukyokai, Gihodo (1969), pp. 27, 61.
3) T. Ozawa, *Bull. Chem. Soc. Jpn.*, **38**, 1881 (1965).
4) H. E. Kissinger, *Anal. Chem.*, **29**, 1702 (1957).
5) A. R. McGhie, P. S. Kalyanaraman, and A. F. Garito, *J. Polym. Sci., Polym. Lett. Ed.*, **16**, 335 (1978).